UCRL-JC-117889

CONF-950226--59

Fast Steering Mirror Systems for the U-AVLIS Program at LLNL

J. Watson, K. Avicola, A. Payne,
R. L. Peterson, and R. Ward

RECEIVED
SEP 09 1996
OSTI

This paper was prepared for submittal to the
SPIE's International Symposia Photonics West '95
San Jose, California
February 4-10, 1995

July 1, 1994

Lawrence Livermore National Laboratory

MASTER

Fast Steering Mirror Systems for the U-AVLIS Program at LLNL

Jim Watson, Ken Avicola, Anthony Payne, Roger L. Peterson,
and Richard Ward

Lawrence Livermore National Laboratory
P.O. Box 808, L-471, Livermore, CA 94550

Abstract

We have successfully deployed several fast steering mirror systems in the Uranium Atomic Vapor Laser Isotope Separation (U-AVLIS) facility at Lawrence Livermore National Laboratory. These systems employ 25mm to 150mm optics and piezoelectric actuators to achieve microradian pointing accuracy with disturbance rejection bandwidths to a few hundred hertz.

1. Introduction

The U-AVLIS facility employs high average power (1-2 kW) pulsed dye lasers operated at high rep rate (several kHz)[1]. Undesired laser beam motion results from a variety of mechanisms including beam induced thermal effects, air turbulence, and vibration from plant support equipment. Thermal effects account for the largest alignment changes, and are corrected with low speed systems using video sensors and stepper motor actuated mirrors. An overview of the beam control and diagnostic systems is given in reference [2]. Additionally, vibration sources inject energy into complex optical transport systems, stimulating natural resonances in optical hardware. Undesired beam motion at frequencies up to a few hundred hertz results from air turbulence and induced vibration. We employ Fast Steering Mirror (FSM) systems to compensate for high speed beam motion. These systems employ piezoelectric actuators for mirror positioning and position sensing diodes (PSD) for error detection. Embedded digital control architecture is used for the systems for maximum flexibility and ease of deployment in each application.

2. FSM Actuators

We are employing two different types of mirror systems in the U-AVLIS facility. For small (25mm-50mm) optic systems, we use a commercially available tilting mirror, the S-330, manufactured by Physik Instrumente (PI) of Germany. This unit was chosen for our application due to the robustness, linearity, and dynamic range of the unit[3]. We have developed drive and control electronics in-house for use with the S-330. This unit exhibits excellent mechanical behavior, and can be accurately modeled as a second order system:

$$G_{(s)}=\frac{K}{S^2+2\zeta\omega_n S+\omega_n^2} \qquad (1)$$

where: S = complex frequency, $\sigma+j\omega$ in rad/sec
ζ = damping, ranging from 0 to 1
ω_n = natural resonant frequency in rad/sec

We have characterized the S-330 using a Tektronix 2642A network analyzer and host software for system identification. System identification provides a model of the FSM in terms of its differential equations, represented in pole-zero form[4]. Figure 1 shows typical position vs. frequency response for the S-330 with a 35mm 6:1 zerodur optic. Given (1), w_n varies typically from 9500 rad/sec to 17k rad/sec for various optics, with z ranging from 0.1 to 0.3.

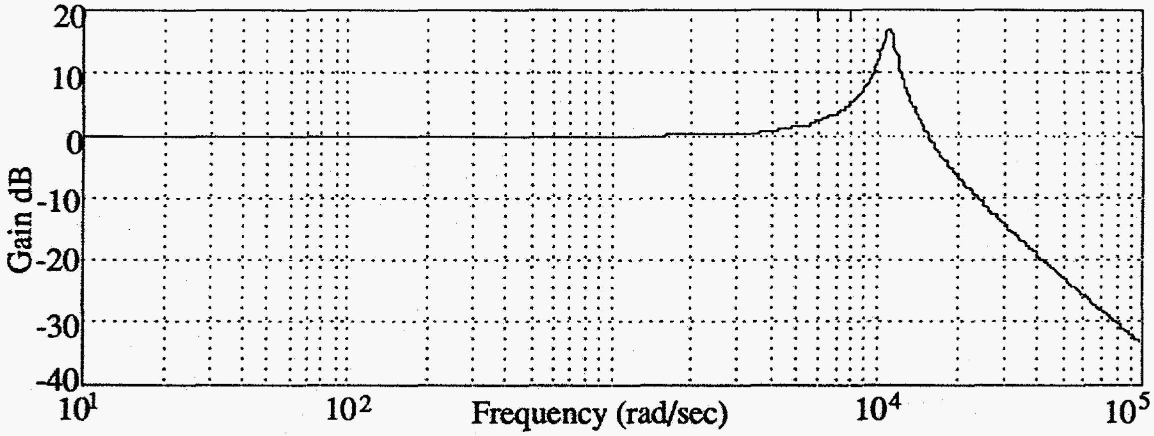

Figure 1 35mm (PI S-330) HBM Actuator Response

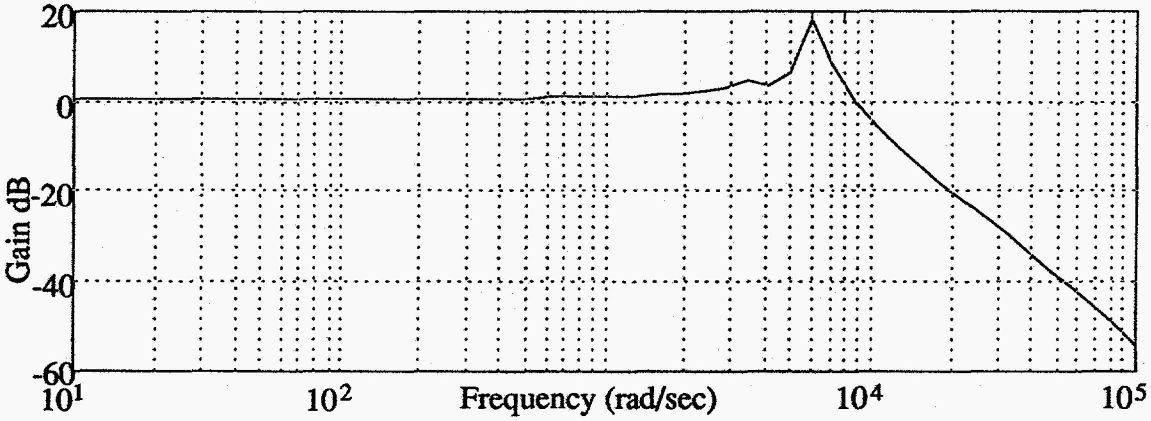

Figure 2 150mm HBM Actuator Response

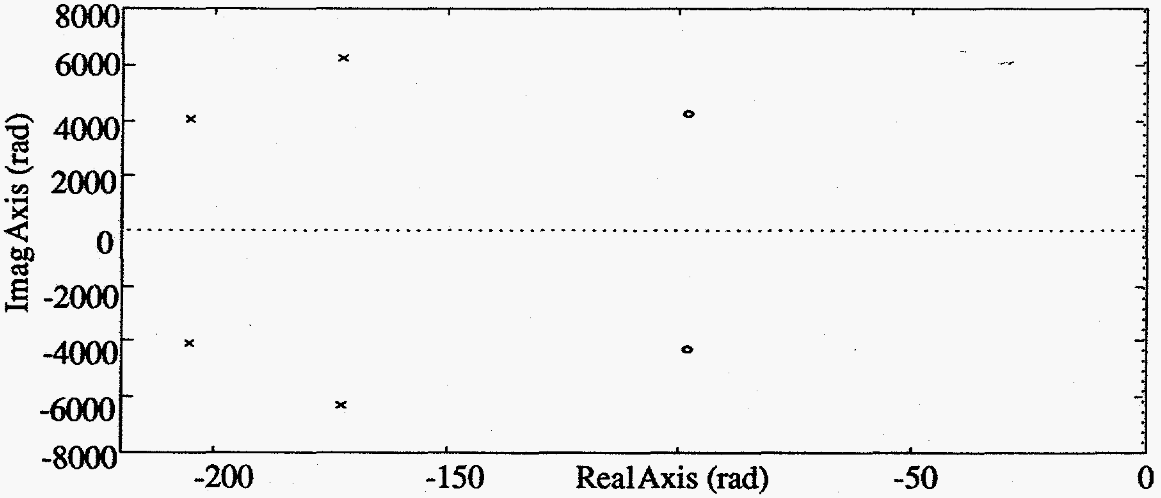

Figure 3 150mm Actuator dominant pole positions

For large (150mm) optics, we have developed a three actuator mirror mount utilizing piezotranslators[5]. This system is inherently more complex, with modes introduced by the transducers, the mirror substrate, and the mount itself. We have characterized this mount with the same procedure used for the PI S-330, and are using a fourth order model for system analysis. Figure 2 shows typical response for the 150 mm FSM while figure 3 identifies dominant pole locations.

3. Controller Architecture

A digital architecture was chosen to provide maximum flexibility in our ever changing plant environment. We currently employ VME-based hardware for a variety of plant control and monitor applications, so this platform was an obvious choice. The controller employs the Motorola MVME 167 68040 CPU, with sample/hold and A/D functions provided by DATEL hardware. Analog signal processing is employed ahead of the A/D. Acromag hardware is used for D/A, and in-house developed amplifiers are used to drive the piezoelectric actuators. Figure 4 shows the controller hardware, along with a functional block diagram.

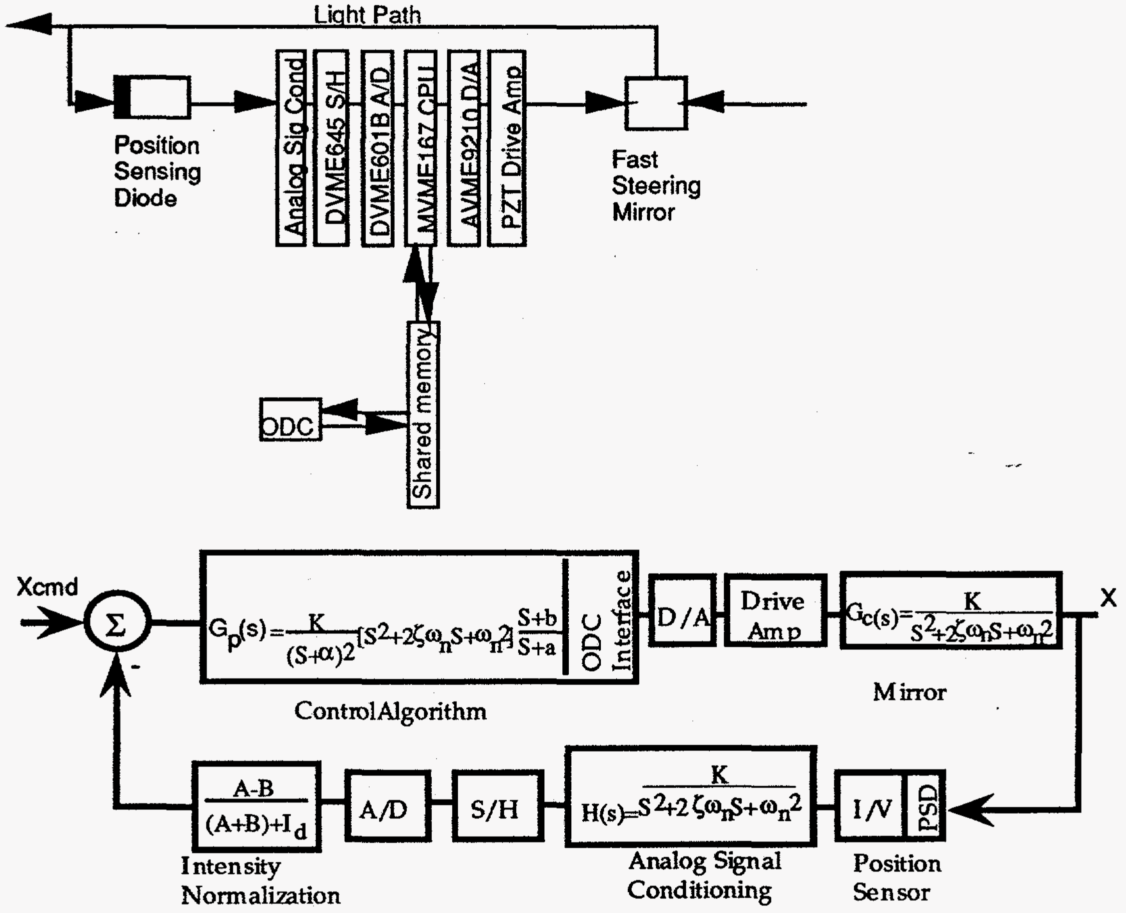

Figure 4 Controller Hardware and Block Diagram

The controller is meant to operate as an embedded (stand alone) system, with minimal user interface. Field parameters such as axis rotation, axis sense, and optical path length (gain) reside in shared memory, and can be user configured by a supervisory control system, such as our Optical Device Controller (ODC). Controller code was developed with ANSI C in Microware's OS-9 environment. Final controller code is burned into ROM and runs in a stand alone fashion with no underlying runtime support.

4. Position Sensor

For laser beam position sensing, we are using the DL10, a 10mm^2 position sensing diode (PSD) from UDT, Inc.[6]. This unit was chosen for responsivity, linearity, and frequency response. The diode signal conditioning electronics employ transimpedance amplifiers and analog summing. As the laser light is pulsed, we employ analog signal conditioning to obtain an average beam position. Judicious pole placement provides optimum averaging without compromising controller performance. The analog conditioning also reduces controller complexity in the digital domain. The gain of the PSD is proportional to light intensity and, therefore, must be normalized. Due to limited dynamic range typical of analog dividers, normalization is performed in the digital domain.

5. Control Algorithms

Algorithm development was accomplished with continuous-time frequency domain models. Development was aided with the use of MATLAB and the MATLAB Control System Toolbox[7]. System identification parameters in pole-zero form were loaded directly from the Tektronix 2642A to a MATLAB compatible file. Gain-phase and evans root-locus analysis techniques were used for controller algorithm development. Controller transfer functions were converted from continuous to discrete time (S to Z) with the use of bilinear transforms and direct pole-zero mapping. Initial controller algorithms employed first order proportional-integral-derivative (PID) architecture:

$$H_{(s)}=\frac{K\omega_d[S^2+\frac{1}{\omega_d}S+\frac{1}{\omega_d\omega_i}]}{S} \qquad (2)$$

As the PID controller is first order, disturbance rejection is limited to 20db/decade below the gain crossover point, and has significant gain above the gain crossover. Further development led to a second order controller:

$$H_{(s)}=\frac{K}{(S+\alpha)^2}[S^2+2\zeta\omega_n S+\omega_n{}^2]\frac{S+b}{S+a} \qquad (3)$$

double real pole complex zero lead-lag

A double pole is used to improve disturbance rejection below the gain crossover point, the complex zero is used to reduce gain above the gain crossover point, and the lead-lag term is used to improve phase margin. This architecture is inherently more stable, as controller roots $(s+\alpha)^2$ are separated from the $j\omega$ axis by α, versus the PID, where a single pole exists at the origin in the s-plane. With the addition of a simple reset routine, the second order controller allows instantaneous recovery from large, unobservable transients and saturation.

6. System Performance and Continuing Work

Figures 5 and 6 show disturbance rejection typical of the second order controller with the 35mm and 150mm FSM. Fielded systems have met all plant performance criteria; however, we plan to continue work on control algorithms to enhance system performance. Discrete system models using MATLAB indicate we are currently limited by the sample-rate of the digital system, which is currently 8kHz. This boundary limits higher order algorithm development with the current generation controller hardware. We have pushed this boundary slightly with analog signal conditioning. However, continued controller enhancement will require higher controller speed.

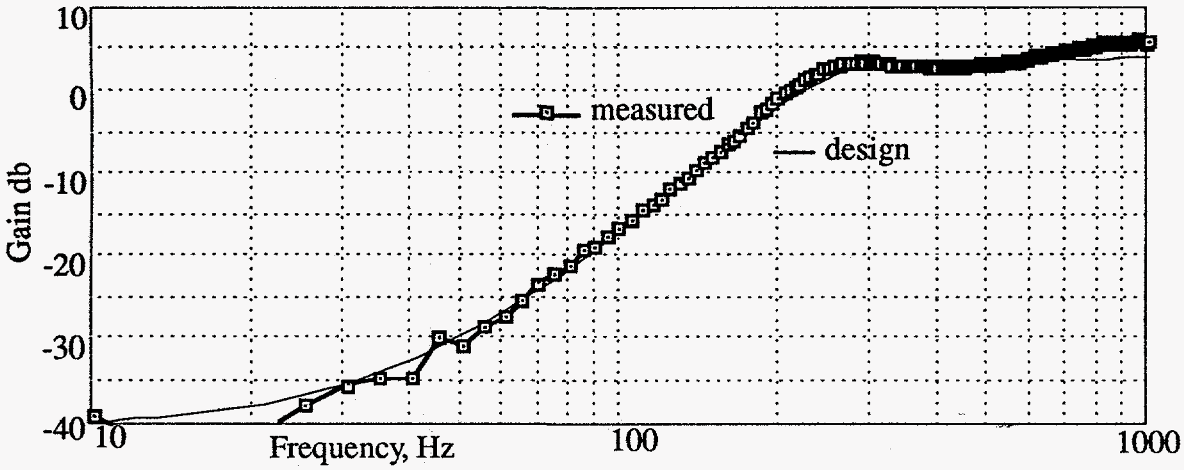

Figure 5 35mm FSM disturbance rejection

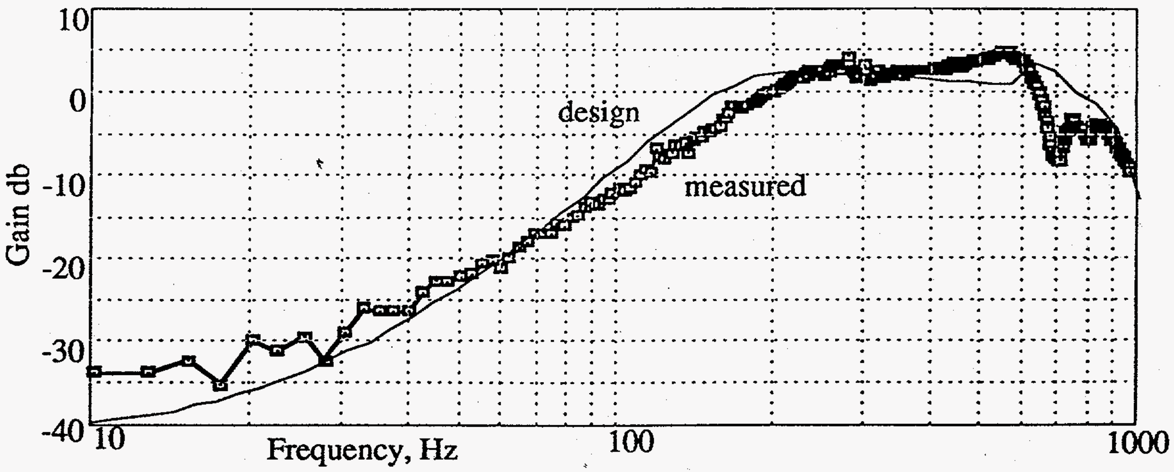

Figure 6 150mm disturbance rejection

7. References

[1] R. H. Hackel and B. E. Warner, *The Copper-Pumped Dye Laser System at Lawrence Livermore National Laboratory* Laser Isotope Separation, SPIE proceedings series Vol. 1859, Society of Photo-Optical Instrumentation Engineers, Bellingham, WA, 1993.

[2] E. S. Bliss, Roger L. Peterson, J. Thaddeus Salmon, and Richard R. Thomas, *Laser Beam Control and Diagnostic System for the Copper-Pumped Dye Laser System at Lawrence Livermore National Laboratory* Laser Isotope Separation, SPIE proceedings series Vol. 1859, Society of Photo-Optical Instrumentation Engineers, Bellingham, WA, 1993.

[3] Physik Instrumente *CAT 109-12/90.15* West Germany.

[4] Benson, D., Techniques *for Signal and System Analysis* Pn 363-0100-01, 1991, Tektronix, Inc.

[5] Bender, D. and Kuklo, T., U.S. *Patent DOE S-75,196* (pending).

[6] UDT Sensors, Inc., *Optoelectronic Components Catalog*, Hawthorne, CA: UDT Inc., 1992.

[7] Grace, A., et al, *Control System Toolbox Users Guide* , Natick, MA: The MathWorks, Inc., 1990.

*This work was performed under the auspices of the U.S. Department of Energy by Lawrence Livermore National Laboratory under contract no. W-7405-Eng-48.